ACS Macro Letters

Letter

pubs.acs.org/macroletters

Electrostatic Assembly of Peptide Nanofiber–Biomimetic Silver Nanowires onto Graphene for Electrochemical Sensors

Jinhui Wang,[†] Xiaojia Zhao,[†] Jingfeng Li,[‡] Xiao Kuang,[∥] Yuqian Fan,[†] Gang Wei,*[,‡] and Zhiqiang Su*[,†]

[†]Beijing Key Laboratory on Preparation and Processing of Novel Polymeric Materials, Beijing University of Chemical Technology, 100029 Beijing, China

[‡]Faculty of Production Engineering, University of Bremen, D-28359 Bremen, Germany

[∥]Beijing National Laboratory for Molecular Sciences, Key Laboratory of Engineering Plastics, Institute of Chemistry, Chinese Academy of Sciences, Beijing 100190, China

Supporting Information

ABSTRACT: Biomacromolecules and their assemblies have the unique ability for biomimetic promotion of the formation of novel and functional nanomaterials. In this work, artificial peptide nanofibers were created with a special designed peptide molecule that contains complex motif sequences and then further metallized to synthesize nanofiber-based silver nanowires. A novel hybrid nanomaterial was obtained successfully by assembling the prepared silver nanowires on graphene nanosheets, and its potential application in nonenzymatic electrochemical H_2O_2 sensing was explored. This fabricated sensor based on graphene and silver nanowires exhibits high sensitivity and selectivity, low detection limit, and wide linear range for the determination of H_2O_2.

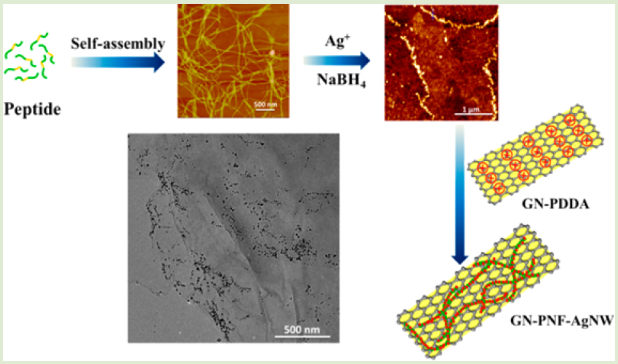

In the past decades, many efforts have been made to explore the organic–inorganic hybrid nanostructures in the field of materials science, biotechnology, and nanotechnology due to their fascinating multiple properties and wide applications.[1] Among them, one-dimensional (1D) nanostructures like nanowires, nanorods, and nanofibers attracted considerable interest.[2] Many 1D inorganic and organic templates, such as carbon nanotubes,[3] DNA,[4] protein nanofibrils,[5] and self-assembled peptide nanofibers (PNFs),[6] have been utilized to synthesize functional 1D nanomaterials. There are 20 natural amino acids that are utilized in the synthesis of peptides, which provide a lot of possibilities to design and synthesize functional PNFs.[7] In recent years, many works on the synthesis of uniform PNFs and their applications in energy materials,[8] biomedicine,[9] highly sensitive sensors,[10] and nanotechnology[6,7,11] have been reported.

Graphene nanosheets (GNs), new two-dimensional (2D) carbon materials with superb conductivity and high surface area, have been widely used for the synthesis of novel hybrid nanomaterials by combining with other nanoscale building blocks.[12] However, it is complex to synthesize GN–metallic nanowire (GN–MNW) hybrids due to the known challenges in the modification of GNs and the conjugation of GNs with MNWs.[13] Specially designed PNFs can present a potential solution to this problem based on two points.[14] First, PNFs are easily modified and bound onto the surface of GNs. For instance, Li and co-workers reported the modification of GNs with self-assembled amyloid fibrils for enzyme sensing.[15] They found that the created amyloid PNF-functionalized GNs could effectively prevent the aggregation of GNs and promote the formation of novel functional materials. Second, PNFs have special biomimetic function for creating metallic nanoparticles (MNPs) with controllable shape and size.[16] For example, Acar et al. found that the self-assembled PNFs can be used as templates for the creation of a 1D gold nanostructure, and the formed gold NPs can be effectively controlled by adjusting the incubation period in ascorbic acid solution.[16b]

H_2O_2 is of great importance in the fields of chemistry, biology, and environmental protection, and many detection techniques for H_2O_2 have been developed.[17] The enzyme-based method is considered to be one of the most attractive approaches for the detection of H_2O_2.[18] However, the relatively high cost, susceptibility to temperature and pH value, and inherent instability are the disadvantages of the enzyme-based sensors.[19] More recently, various noble metal-based nanohybrids have been applied to construct a nonenzymatic H_2O_2 sensor.[12b,20] Among them, Ag is much cheaper than the other metals mentioned above and maintains excellent electrochemical properties for the reduction of H_2O_2.[21] In addition, silver nanowires (AgNWs) have high aspect ratio and superior optical and electrical performances. Therefore, the combination

Received: April 9, 2014
Accepted: May 20, 2014
Published: May 22, 2014

   dx.doi.org/10.1021/mz500213w | *ACS Macro Lett.* 2014, 3, 529–533

of AgNWs with GNs makes it possible to produce novel functional nanomaterials and nanodevices.[22]

Herein, we demonstrated the creation of a novel PNF by controlling the self-assembly of a specifically designed peptide with three functional motifs on both sides and the center part of the peptide chain. Furthermore, we reported the synthesis of biomimetic AgNWs templated by PNFs (PNF-AgNW) and the subsequent electrostatic assembly of the synthesized PNF-AgNW onto GNs to fabricate GN−PNF-AgNW nanohybrids. The potential application of the created GN−PNF-AgNW nanohybrids for electrochemical sensing of H_2O_2 was further explored. The strategy for creating AgNWs onto GNs presented in this work is green and very effective, and the prepared GN−PNF-AgNW nanohybrid-based electrochemical sensor shows enhanced performance for the determination of H_2O_2.

Figure 1 shows a schematic representation for the synthesis of GN−PNF-AgNW nanohybrids by electrostatic assembling

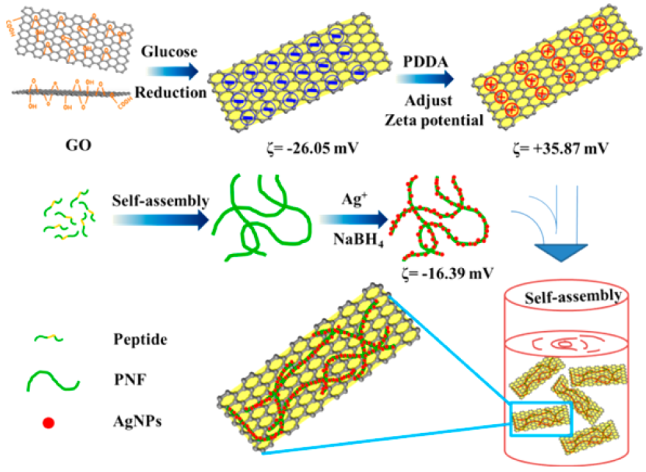

Figure 1. Schematic representation for the formation of PNF bioinspired AgNWs on GNs.

PNF-AgNW nanohybrids onto polymer-modified GNs (detailed information in Supporting Information). First, graphene oxide (GO) nanosheets were chemically reduced into GNs by glucose,[23] and the zeta potential of the obtained GNs was −26.05 mV. Second, the synthesized GNs were modified with a positive-charged polymer, poly(diallyldimethylammonium chloride) (PDDA), to obtain PDDA-GNs with a zeta potential of +35.87 mV. Third, PNFs were created by controlling the self-assembly of the specifically designed peptide molecules, and the synthesized artificial PNFs inspired the formation of PNF-AgNW nanohybrids with a zeta potential of −16.39 mV. Finally, PNF-AgNW nanohybrids were bound onto the surface of GNs by the electrostatic interaction due to the big gap of their zeta potentials (−16.39 vs +35.87 mV).

Figure 2a shows the molecular model and amino acid sequence of the multifunctional peptide used in this work. This specifically designed peptide has two functions. The head and tail motif sequences (VIA) enable the self-assembly of peptide to form PNFs. It has been reported that the water-soluble tripeptide (H_2N-VIA-COOH) can form straight and unbranched PNFs by the intermolecularly hydrogen-bond-induced β-sheet self-assembly.[24] The center motif sequence (GASLWWSEKL) is related to the biomimetic synthesis of MNPs. A previous report has indicated that this sequence has

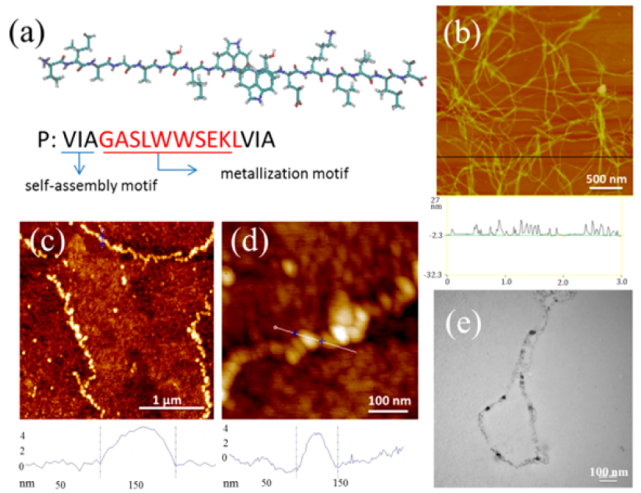

Figure 2. Self-assembly and metallization of PNFs: (a) Molecular model and motif sequences of peptide molecule. (b) AFM image of the self-assembled PNFs. (c) Low- and (d) high-magnified AFM. (e) TEM images of PNFs after metallization (PNF-AgNW).

the ability to control the size and shape of synthesized NPs.[25] Although the separated sequence has the unique function, it is still unknown if the complex motif sequences can preserve these two important functions. To make it clear, we explored the formation of PNFs in various experimental conditions by adjusting the temperature, pH value, incubation period, and ethanol concentration. We found that uniform PNFs were created by incubating 40 ng μL^{-1} of peptide in 20% ethanol at both room temperature and 37 °C for 5 days (details in the Supporting Information), and the typical AFM height image of the created PNFs is shown in Figure 2b and Figure S1 (Supporting Information). We suggest that the ethanol mediates the conformation transition of peptide molecules to form β-sheet structure and promotes the formation of linear PNFs.[5a] It can be observed that the created PNFs display a smooth surface with a height of 4.0 ± 1.0 nm and length up to several micrometers. It should be noted that some parameters, like solvent, peptide concentration, temperature, and incubation period, may have to be fine-tuned to control the self-assembly and formation of PNFs. Further investigation on the self-assembly mechanism and kinetics of peptide molecules with circular dichroism is needed.

After metallization, we found that a large number of Ag NPs deposited on the surface of PNFs uniformly by in situ reduction of Ag^+ and the PNF-based AgNWs were created successfully, as shown in the AFM images in Figure 2c and d. The corresponding section analyses indicate the height of AgNPs was approximately 5.2 ± 0.5 nm. In addition, no obvious agglomerations were found in both images, which prove the excellent shape and size control abilities of our peptide. TEM characterization further confirmed the formation of PNF-AgNW nanohybrids (Figure 2e).

To conjugate the created PNF-AgNW nanohybrids onto GNs, the GNs were first modified with PDDA (cationic polyelectrolyte) to provide a positive zeta potential. Figure S2a (Supporting Information) shows the typical AFM image of PDDA-modified GNs. Compared to the glucose-reduced GNs (Figure S2b, Supporting Information), the PDDA-modified GNs show larger surface roughness, which is ascribed to the binding of PDDA with GNs.[26] After that, PNF-AgNW can then be bound onto the GNs to form GN−PNF-AgNW nano-

dx.doi.org/10.1021/mz500213w | ACS Macro Lett. 2014, 3, 529−533

hybrids via the electrostatic interaction. Figure 3a and b present the typical TEM images of the synthesized GN−PNF-AgNW

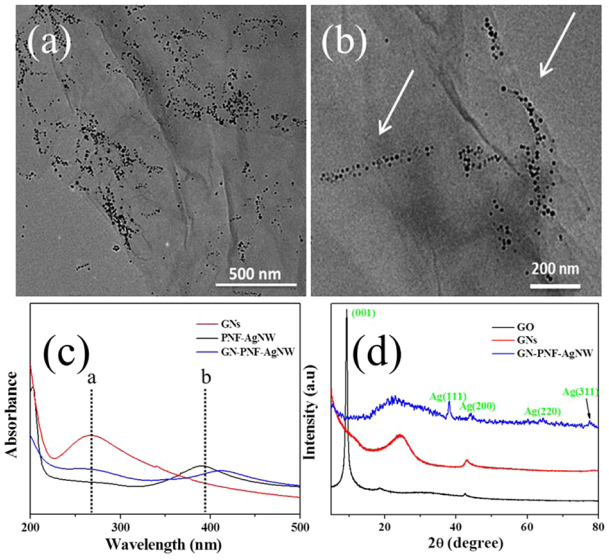

Figure 3. Characterizations of GN−PNF-AgNW nanohybrids: (a, b) TEM images with different magnifications. (c) UV−vis spectra of GNs, AgNPs, PNF-AgNP, and GN−PNF-AgNW. (d) XRD patterns of GO, GNs, and GN−PNF-AgNW nanohybrids.

nanohybrids with different magnifications. It can be found that some linear AgNP arrays (named as AgNWs) were formed on the surface of GNs, as indicated with arrows in Figure 3b. The diameter of synthesized AgNPs was measured to be 6.5 ± 1.7 nm, which is similar to the height data obtained by AFM (5.2 ± 0.5 nm). The synthesized GN−PNF-AgNW nanohybrids were observed by AFM as well, and we also found the conjugation of PNF-AgNW nanohybrids with GNs (Figure S3, Supporting Information).

The successful preparation of GN−PNF-AgNW nanohybrids was confirmed by the UV−vis absorption spectrum (Figure 3c). Previous work indicates that GO exhibits strong bands centered at 227 and 300 nm, and glucose-reduced GN has a characteristic absorption peak at 267 nm.[22] Compared to the absorption peak of PNF-AgNW at 391 nm, it is found that the absorption peak of GN−PNF-AgNW exhibits a big red shift to 410 nm, which is ascribed to the binding of PNF-AgNW with GNs. The synthesized GO, GNs, and GN−PNF-AgNW nanohybrids were further measured with X-ray diffraction (XRD), and their XRD patterns are shown in Figure 3d. After reduction with glucose, a broad peak around 24° appeared, and the peak of GO at 9.35° disappeared, indicating the successful reduction of GO into GN.[27] In addition, according to the JCPDS (No. 65-2871), the (111), (220), and (331) peaks in the XRD pattern of GN−PNF-AgNW correspond to the principal reflections of Ag NPs. XPS characterization further proves the formation of GN−PNF-AgNW nanohybrids (Figure S4a−d, Supporting Information).

On the basis of the synthesized GN−PNF-AgNW nanohybrids, we constructed a nonenzymatic electrochemical H_2O_2 sensor by immobilizing the aqueous dispersion of the created nanohybrids onto a glassy carbon electrode (GCE). Figure 4a shows the electrochemical responses of the bare GCE and GCEs modified with GN-PDDA and GN−PNF-AgNW nanohybrids in 0.2 M N_2-saturated phosphate-buffered saline

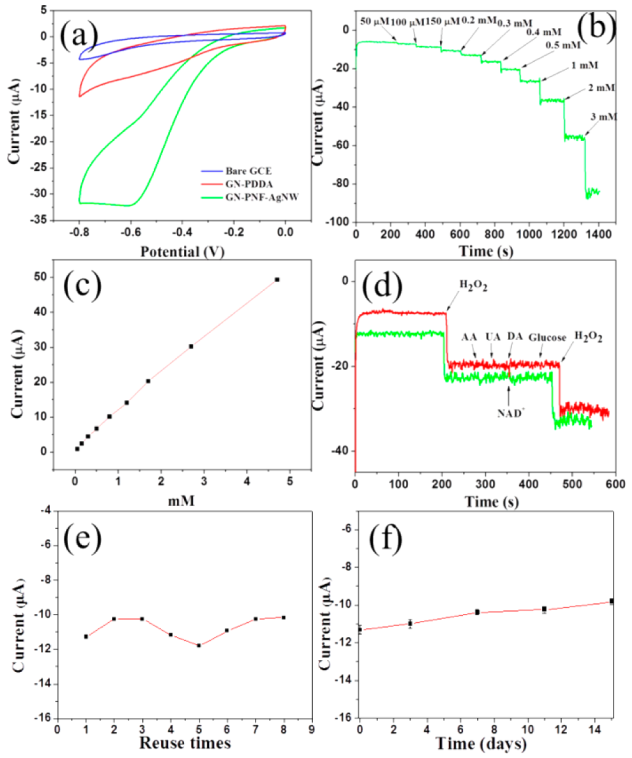

Figure 4. Electrochemical H_2O_2 sensing: (a) CVs of GCEs modified with GN-PDDA and GN−PNF-AgNW nanohybrids in H_2O_2. (b) $I-T$ response of GN−PNF-AgNW/GCE in 0.2 M PBS with successive addition of H_2O_2 at −0.6 V. (c) Calibrated line. (d) Selectivity. (e) Reuse ability. (f) Long-term stability.

(PBS, pH = 6.5) in the presence of 5.0 mM H_2O_2. It can be seen that the pure GCE shows no obvious redox process. When the GCE was modified with GN-PDDA, the diffused current increased and still no obvious redox peak can be observed. In contrast, the reduction current of GN−PNF-AgNW-modified GCE shows a great peak with an intensity of about 32 μA at −0.6 V. All these observations indicate that the AgNWs exhibit significant electrochemical activity for H_2O_2 reduction. In addition, we suggest that the enhanced electrochemical property of GN−PNF-AgNW is in some way ascribed to the high surface area volume ratio of the 2D GNs. Herein, −0.6 V was selected as the applied potential for $I-T$ measurement in this work. Figure 4b shows the typical $I-T$ plot of the synthesized GN−PNF-AgNW-modified GCE on successive addition of H_2O_2 with different concentrations. When H_2O_2 was added into the PBS under stirring, the modified GCE could reach the maximum steady-state current rapidly. The steady-state calibration curve of the modified GCE (Figure 4c) indicates a linear response to H_2O_2, and the linear detection range is observed to be approximately from 50 μM to 5 mM (R = 0.9977, S/N = 3). The detection limit of this sensor is calculated to be 10.4 μM.

The selectivity and anti-interference of the fabricated electrochemical sensor were evaluated first by adding ascorbic acid (AA), uric acid (UA), dopamine (DA), and glucose into the system. It can be found that no interference was observed at the applied potential (red line in Figure 4d), which is similar to our previous report on the H_2O_2 sensor.[28] To check the potential interference of the electron acceptor on this sensor, β-nicotinamide adenine dinucleotide (NAD^+) was selected and added into the system. Figure 4d (green line) presents the

dx.doi.org/10.1021/mz500213w | ACS Macro Lett. 2014, 3, 529−533

amperometric response of GN−PNF-AgNW-modified GCE for the successive addition of 1 mM H_2O_2, 0.6 mM NAD^+, and 1 mM H_2O_2. It can be seen that negligible interference was observed at the applied potential. Therefore, the high selectivity of our sensor was identified.

The reuse stability of the fabricated GN−PNF-AgNW-modified GCE was further examined (Figure 4e), and the result shows that the repeated usage of the created sensor is possible for at least 8 times. Significant reduction in current after 8 times of use is displayed, which is possible ascribed to the detachment of the GN−PNF-AgNW nanohybrids from the electrode. Finally, the long-term stability of the modified GCE was explored over a 15-day period (Figure 4f). The prepared electrode was stored in a refrigerator at 4 °C and measured every 3−4 days. The result shows that the reduction current response retains more than 87% of its initial value in response to 1 mM H_2O_2 after 15 days, indicating an acceptable stability of our GN−PNF-AgNW-based sensor.

In conclusion, we demonstrated the creation of a novel PNF by controlling the self-assembly of a specifically designed functional peptide. The designed peptide reveals two unique abilities: not only creating the 1D PNFs by self-assembly but also promoting the formation of AgNWs by metallization. Furthermore, the GN−PNF-AgNW nanohybrids were successfully synthesized by electrostatic assembling the negative-charged PNF-AgNW onto the positive-charged PDDA-modified GNs, and the created GN−PNF-AgNW nanohybrids were utilized to fabricate a nonenzymatic electrochemical H_2O_2 sensor with enhanced performances. To the best of our knowledge, this is the first report on the preparation of self-assembled PNFs with multifunctional peptides and the formation of AgNWs on GNs with the inspiration of PNFs. It is expected that the synthesized GN−PNF-AgNW nanohybrids will have other potential applications in nanodevices, biomedicine, antimicrobial materials, and Raman analysis.

■ ASSOCIATED CONTENT

Supporting Information

Preparation of PNFs, PNF-AgNW, and GN−PNF-AgNW nanohybrids; AFM and XPS characterization; electrochemical measurements. This material is available free of charge via the Internet at http://pubs.acs.org.

■ AUTHOR INFORMATION

Corresponding Authors

*E-mail: wei@uni-bremen.de (G. Wei).
*E-mail: suzq@mail.buct.edu.cn (Z. Su).

Author Contributions

The manuscript was written through contributions of all authors. All authors have given approval to the final version of the manuscript.

Notes

The authors declare no competing financial interest.

■ ACKNOWLEDGMENTS

We acknowledge the financial support from the Fundamental Research Funds for the Central Universities (Project No. ZZ1307). We would like to thank the financial support of the China Scholarship Council (CSC) PhD scholarship.

■ REFERENCES

(1) (a) Li, X.; Qin, Y.; Picraux, S. T.; Guo, Z. X. J. *Mater. Chem.* **2011**, *21*, 7527−7547. (b) Sanchez, C.; Belleville, P.; Popall, M.; Nicole, L. *Chem. Soc. Rev.* **2011**, *40*, 696−753. (c) Dolbecq, A.; Dumas, E.; Mayer, C. R.; Mialane, P. *Chem. Rev.* **2010**, *110*, 6009−6048.

(2) (a) Feigel, I. M.; Vedala, H.; Star, A. *J. Mater. Chem.* **2011**, *21*, 8940−8954. (b) Wanekaya, A. K.; Chen, W.; Myung, N. V.; Mulchandani, A. *Electroanalysis* **2006**, *18*, 533−550. (c) Liang, H. W.; Liu, S.; Yu, S. H. *Adv. Mater.* **2010**, *22*, 3925−3937.

(3) (a) Wei, G.; Xu, F.; Li, Z.; Jandt, K. D. *J. Phys. Chem. C* **2011**, *115*, 11453−11460. (b) Kim, S. W.; Ryu, J.; Park, C. B.; Kang, K. *Chem. Commun.* **2010**, *46*, 7409−7411.

(4) (a) Wang, F.; Willner, B.; Willner, I. *Curr. Opin. Biotechnol.* **2013**, *24*, 562−574. (b) Willner, I.; Willner, B. *Nano Lett.* **2010**, *10*, 3805−3815.

(5) (a) Wei, G.; Reichert, J.; Jandt, K. D. *Chem. Commun.* **2008**, *44*, 3903−3905. (b) Scheibel, T. *Curr. Opin. Biotechnol.* **2005**, *16*, 427−433.

(6) (a) Shiba, K. *Curr. Opin. Biotechnol.* **2010**, *21*, 412−425. (b) Yang, Y.; Khoe, U.; Wang, X.; Horii, A.; Yokoi, H.; Zhang, S. *Nano Today* **2009**, *4*, 193−210.

(7) Ulijn, R. V.; Smith, A. M. *Chem. Soc. Rev.* **2008**, *37*, 664−675.

(8) Ryu, J.; Kim, S. W.; Kang, K.; Park, C. B. *Adv. Mater.* **2010**, *22*, 5537−5541.

(9) (a) Jun, H. W.; Paramonov, S. E.; Hartgerink, J. D. *Soft Matter* **2006**, *2*, 177−181. (b) Loo, Y.; Zhang, S.; Hauser, C. A. E. *Biotechnol. Adv.* **2012**, *30*, 593−603.

(10) Kim, J. H.; Lim, S. Y.; Nam, D. H.; Ryu, H. S.; Ku, H.; Park, C. B. *Biosens. Bioelectron* **2011**, *26*, 1860−1865.

(11) Khalily, M. A.; Ustahuseyin, O.; Garifullin, R.; Genc, R.; Guler, M. O. *Chem. Commun.* **2012**, *48*, 11358−11360.

(12) (a) Zhao, X.; Li, Yang.; Wang, J.; Ouyang, Z.; Li, J.; Wei, G.; Su, Z. *ACS Appl. Mater. Interfaces* **2014**, *6*, 4254−4263. (b) Zhang, P.; Zhang, X.; Zhang, S.; Lu, X.; Li, Q.; Su, Z.; Wei, G. *J. Mater. Chem. B* **2013**, *1*, 6525−6531. (c) Wei, G.; Zhang, Y.; Steckbeck, S.; Su, Z.; Li, Z. *J. Mater. Chem.* **2012**, *22*, 17190−17195. (d) Ling, S.; Li, C.; Adamcik, J.; Wang, S.; Shao, Z.; Chen, X.; Mezzenga, R. *ACS Macro Lett.* **2014**, *3*, 146−152.

(13) (a) Luan, V. H.; Tien, H. N.; Cuong, T. V.; Kong, B. S.; Chung, J. S.; Kim, E. J.; Hur, S. H. *J. Mater. Chem.* **2012**, *22*, 8649−8653. (b) Tien, H. W.; Hsiao, S. T.; Liao, W. H.; Yu, Y. H.; Lin, F. C.; Wang, Y. S.; Li, S. M.; Ma, C. C. M. *Carbon* **2013**, *58*, 198−207.

(14) (a) Adhikari, B.; Banerjee, A. *Soft Matter* **2011**, *7*, 9259−9266. (b) Wang, Y.; Cao, L. C.; Guan, S.; Shi, G.; Luo, Q.; Thistlethwaite, I.; Huang, Z.; Xu, J.; Liu, J. *J. Mater. Chem.* **2012**, *22*, 2575−2681.

(15) Li, C.; Adamcik, J.; Mezzenga, R. *Nat. Nanotechnol.* **2012**, *7*, 421−427.

(16) (a) Reches, M.; Gazit, E. *Science* **2003**, *300*, 625−627. (b) Acar, H.; Genc, R.; Urel, M.; Erkal, T. S.; Dana, A.; Guler, M. O. *Langmuir* **2012**, *28*, 16347−16354.

(17) (a) Klassen, N. V.; Marchington, D.; McGowan, H. C. E. *Anal. Chem.* **1994**, *66*, 2921−2925. (b) Chang, M. C. Y.; Pralle, A.; Isacoff, E. Y.; Chang, C. J. *J. Am. Chem. Soc.* **2004**, *126*, 15392−15393. (c) Shu, X.; Chen, Y.; Yuan, H.; Gao, S.; Xiao, D. *Anal. Chem.* **2007**, *79*, 3695−3702. (d) Wang, B.; Zhang, J.; Pan, Z.; Tao, X.; Wang, H. *Biosens. Bioelectron.* **2009**, *24*, 1141−1145.

(18) (a) Trifonov, A.; Tel-Vered, R.; Yehezkeli, O.; Woerner, M.; Willner, I. *ACS Nano* **2013**, *7*, 11358−11368. (b) Pelossof, G.; Tel-Vered, R.; Elbaz, J.; Willner, I. *Anal. Chem.* **2010**, *82*, 4396−4402.

(19) Zou, G.; Ju, H. *Anal. Chem.* **2004**, *76*, 6871−6876.

(20) (a) Polsky, R.; Gill, R.; Kaganovsky, L.; Willner, I. *Anal. Chem.* **2006**, *78*, 2268−2271. (b) Chen, S.; Yuan, R.; Chai, Y.; Hu, F. *Microchim. Acta* **2013**, *180*, 15−32.

(21) Riskin, M.; Tel-Vered, R.; Willner, I. *Adv. Funct. Mater.* **2009**, *19*, 2474−2480.

(22) (a) Lee, D.; Lee, H.; Ahn, Y.; Jeong, Y.; Lee, D. Y.; Lee, Y. *Nanoscale* **2013**, *5*, 7750−7755. (b) Liu, Y.; Chang, Q.; Huang, L. *J. Mater. Chem. C* **2013**, *1*, 2970−2974.

(23) Guo, Y.; Guo, S.; Ren, J.; Zhai, J.; Dong, S.; Wang, E. *ACS Nano* **2010**, *4*, 4001−4010.
(24) Ray, S.; Das, A. K.; Drew, M. G. B.; Banerjee, A. *Chem. Commun.* **2006**, *42*, 4230−4232.
(25) Tan, Y. N.; Lee, J. Y.; Wang, D. I. C. *J. Am. Chem. Soc.* **2010**, *132*, 5677−5686.
(26) Ren, W.; Fang, Y.; Wang, E. *ACS Nano* **2011**, *5*, 6425−6433.
(27) Liu, S.; Tian, J.; Wang, L.; Li, H.; Zhang, Y.; Sun, X. *Macromolecules* **2010**, *43*, 10078−10083.
(28) Ouyang, Z.; Li, J.; Wang, J.; Li, Q.; Ni, T.; Zhang, X.; Wang, H.; Li, Q.; Su, Z.; Wei, G. *J. Mater. Chem. B* **2013**, *1*, 2415−2424.